

REGULARIZED MR COIL SENSITIVITY ESTIMATION USING AUGMENTED LAGRANGIAN METHODS

Michael J. Allison, Sathish Ramani, Jeffrey A. Fessler

University of Michigan
Department of Electrical Engineering and Computer Science
Ann Arbor, MI, USA

ABSTRACT

Several magnetic resonance (MR) parallel imaging techniques require explicit estimates of the receive coil sensitivity profiles. These estimates must be accurate over both the object and its surrounding regions to avoid generating artifacts in the reconstructed images. Statistical estimation methods provide robust sensitivity estimates but can be computationally expensive. In this paper, we propose an augmented Lagrangian (AL) based method that estimates the coil sensitivity by minimizing a quadratic cost function. This method reformulates the finite differencing matrix to allow for exact alternating minimization steps. We also explore a variation of our algorithm that involves intermediate updating of the Lagrange multipliers. We demonstrate that our proposed algorithm converges in half the time of the traditional conjugate gradient method with a circulant preconditioner (PCG) on a real data set.

Index Terms— coil sensitivity, augmented Lagrangian, quadratic minimization, finite differences, parallel imaging

1. INTRODUCTION

Accurate radio-frequency coil sensitivity profiles are required in many parallel imaging applications (e.g., [1]). Due to coil deformation during patient setup and dielectric coupling, these profiles must be determined at the time of acquisition [2]. One common approach is to perform a calibration scan prior to the parallel imaging acquisition in which images from a large body coil and multiple surface coils are acquired and reconstructed. Since the body coil has near uniform sensitivity, its image can be used in conjunction with a surface coil image to estimate the surface coil sensitivity profile.

The most straightforward method to estimate the coil sensitivity is to compute the ratio of the surface coil image voxel values (z_i) to the body coil image voxel values (y_i), z_i/y_i . Typically, such estimates are corrupted due to measurement noise, particularly in regions of low signal. Furthermore, ratio estimates have sharp discontinuities at object edges, contrary to the smooth nature of true coil sensitivity profiles [3]. It is also important to have accurate sensitivity estimates in any low signal regions surrounding the object to avoid reconstruction artifacts that could arise due to patient motion [4]. The ratio estimator, however, does not extrapolate; thus, more advanced estimation methods are required.

One approach to generate smoother sensitivity estimates is to measure only the center of k -space. Although simple, this approach does not accurately estimate the sensitivity near object edges and can introduce Gibbs ringing artifacts. Filtering procedures have also

been proposed including polynomial fitting (see [3, 5]), wavelet denoising [6], and using thin-plate splines [7]. Yet these methods fail to completely eliminate the Gibbs ringing, while selecting a particular basis function is complicated by the varying size of low signal regions within the images [3]. Furthermore, many of these methods disregard the non-stationary variance of the noise in the sensitivity estimates. Alternatively, statistical estimation methods [3, 8] provide smooth estimates and are capable of extrapolation without the need for basis function selection and explicit filtering. These methods, however, can be computationally expensive [3] and this cost is compounded by the large number of coils in some arrays.

In this paper, we take a statistical approach and pose sensitivity estimation as the minimization of a quadratic cost function like in [3]. The large matrices in the cost function prevent one from computing a simple, direct solution to this problem. Instead, iterative methods must be used for large data sets. Due to the slow convergence time of traditional methods like conjugate gradient (CG), we previously investigated an AL based method to minimize the cost function [9]. However, that method was complicated by an approximate minimization step and its final convergence speed was similar to that of PCG with a circulant preconditioner. We therefore propose a new AL based estimation method that uses exact alternating minimization steps. This approach is made possible by separating the finite differencing matrix into two matrices with more exploitable structures. We also explore updating the Lagrange multipliers between alternating minimization steps. Our improved algorithm, AL-Circ, yields accurate estimates in half the time of PCG.

2. METHODS

This section introduces our method for MR coil sensitivity estimation. We begin by posing the estimator as an optimization problem. We then outline the general approach used to solve this problem and present the specific algorithm in detail.

2.1. Cost Function Formulation

Statistical methods for MR coil sensitivity estimation are both robust to noise and effective at extrapolating the estimate in regions of low signal [3]. These methods avoid computing the quotient (z_i/y_i) by expressing the problem as the minimization of a cost function containing a data-fidelity term and a regularization term that promotes smoothness in the estimate. Similar to [3], we estimate the sensitivity profile by minimizing a weighted sum of quadratic terms:

$$\hat{\mathbf{s}} \triangleq \arg \min_{\mathbf{s}} \frac{1}{2} \|\mathbf{z} - \mathbf{D}\mathbf{s}\|_2^2 + \frac{\lambda}{2} \|\mathbf{R}\mathbf{s}\|_2^2, \quad (1)$$

The authors would like to thank NSERC and NIH-CA87634 for funding support and Marko Ivancevic for acquiring the breast phantom data.

where $\mathbf{s} = [s_1, \dots, s_N]^T$ with $s_i \in \mathbb{C}$ being the desired coil sensitivity at the i th voxel, $\mathbf{z} = [z_1, \dots, z_N]^T$ with $z_i \in \mathbb{C}$ being the surface coil image value at the i th voxel, $\mathbf{D} = \text{diag}\{y_i m_i\}$ is a diagonal matrix containing the body coil image voxel values ($y_i \in \mathbb{C}$) multiplied by the corresponding values of a binary mask specifying voxels with significant intensities (m_i), $\mathbf{R} \in \mathbb{R}^{M \times N}$ is a finite differencing matrix with non-periodic boundaries, and $\lambda > 0$ is a regularization coefficient. The inclusion of a mask ensures that the estimate is based primarily on pixels that provide meaningful sensitivity information.

Equation (1) is quadratic and therefore has a closed-form solution; however, computing this solution is impractical due to the size and complexity of \mathbf{R} . Memory constraints further restrict the use of other direct methods, such as Cholesky factorization, for large problems like 3D data sets. Furthermore, standard iterative solution methods such as CG exhibit slow converge for this problem even when using carefully selected preconditioners. To address this, we propose an AL based method to minimize the cost function.

2.2. Overview of Augmented Lagrangian Approach

Augmented Lagrangian based minimization techniques have been used to accelerate convergence in imaging problems such as denoising and reconstruction (see [10]). The focus of that work has been on problems that contain non-differentiable regularization terms such as those based on the ℓ_1 -norm. However, the underlying theory applies to a wide variety of optimization problems including our own. We therefore follow a similar approach, with the development of our algorithm consisting of three stages [10]. First, we reformulate the finite differencing matrix and use variable splitting to convert the unconstrained optimization problem into an equivalent constrained problem. Second, we introduce vector Lagrange multipliers and express the constrained problem in an AL framework. Third, we solve the resulting AL problem using an alternating minimization scheme.

2.3. AL-Circ Method

The drawback of our previous algorithm [9] was that it required an approximate PCG solution for one of the alternating minimization steps. We can avoid such a step by expressing the finite differencing matrix as $\mathbf{R} = \mathbf{B}\mathbf{C}$ where $\mathbf{C} \in \mathbb{R}^{M \times N}$ is a typical finite differencing matrix but with additional non-zero rows that penalize the differences between pixels on opposing edges of the image and \mathbf{B} is a diagonal matrix that contains a binary mask to eliminate the effects of these added rows. Unlike \mathbf{R} , the additional rows in \mathbf{C} ensure that $\mathbf{C}^H \mathbf{C}$ is block circulant with circulant blocks. Figure 1 presents an illustration of these matrices for the case of 1D first-order finite differences. We then re-express the estimation problem in (1) as

$$\hat{\mathbf{s}} = \arg \min_{\mathbf{s}} \frac{1}{2} \|\mathbf{z} - \mathbf{D}\mathbf{s}\|_2^2 + \frac{\lambda}{2} \|\mathbf{B}\mathbf{C}\mathbf{s}\|_2^2. \quad (2)$$

Next, we introduce two splitting variables, $\mathbf{u}_0 \in \mathbb{C}^M$ and $\mathbf{u}_1 \in \mathbb{C}^N$, to this new formulation to decouple the matrices \mathbf{D} , \mathbf{B} , and \mathbf{C} . The resulting constrained optimization problem is

$$\arg \min_{\mathbf{s}, \mathbf{u}_0, \mathbf{u}_1} \Psi(\mathbf{s}, \mathbf{u}_0) \quad \text{s.t.} \quad \mathbf{u}_0 = \mathbf{C}\mathbf{u}_1 \quad \text{and} \quad \mathbf{u}_1 = \mathbf{s}, \quad (3)$$

where $\Psi(\mathbf{s}, \mathbf{u}_0) \triangleq \frac{1}{2} \|\mathbf{z} - \mathbf{D}\mathbf{s}\|_2^2 + \frac{\lambda}{2} \|\mathbf{B}\mathbf{u}_0\|_2^2$. We then tackle (3) using an AL formalism [10] that leads to the following AL function-based minimization problem:

$$\arg \min_{\mathbf{s}, \mathbf{u}_0, \mathbf{u}_1} \Psi(\mathbf{s}, \mathbf{u}_0) + \frac{\nu_0}{2} \|\mathbf{u}_0 - \mathbf{C}\mathbf{u}_1 - \boldsymbol{\eta}_0\|_2^2 + \frac{\nu_1}{2} \|\mathbf{u}_1 - \mathbf{s} - \boldsymbol{\eta}_1\|_2^2, \quad (4)$$

$$\underbrace{\begin{bmatrix} 0 & 0 & 0 & 0 & 0 \\ -1 & 1 & 0 & 0 & 0 \\ 0 & -1 & 1 & 0 & \dots \\ 0 & 0 & -1 & 1 & 0 \end{bmatrix}}_{\mathbf{R}} = \underbrace{\begin{bmatrix} 0 & 0 & 0 & 0 & 0 \\ 0 & 1 & 0 & 0 & 0 \\ 0 & 0 & 1 & 0 & \dots \\ 0 & 0 & 0 & 1 & 0 \end{bmatrix}}_{\mathbf{B}} \underbrace{\begin{bmatrix} 1 & 0 & 0 & 0 & -1 \\ -1 & 1 & 0 & 0 & 0 \\ 0 & -1 & 1 & 0 & \dots \\ 0 & 0 & -1 & 1 & 0 \end{bmatrix}}_{\mathbf{C}}$$

Fig. 1. The upper portion of the matrices \mathbf{R} , \mathbf{B} , and \mathbf{C} for the case of 1D first-order finite differences. Note that the top row of \mathbf{C} computes the difference between the first and last pixels, hence the need for the mask \mathbf{B} .

where $\boldsymbol{\eta}_0 \in \mathbb{C}^M$ and $\boldsymbol{\eta}_1 \in \mathbb{C}^N$ are vectors of Lagrange multipliers and $\nu_0, \nu_1 > 0$ are additional parameters that influence the convergence rate but do not affect the final estimate.

Due to the complexity of jointly minimizing (4) over \mathbf{s} , \mathbf{u}_0 , and \mathbf{u}_1 , we consider an alternating minimization scheme. In particular, we sequentially solve

$$\mathbf{s}^{(j+1)} = \arg \min_{\mathbf{s}} \frac{1}{2} \|\mathbf{z} - \mathbf{D}\mathbf{s}\|_2^2 + \frac{\nu_1}{2} \|\mathbf{u}_1^{(j)} - \mathbf{s} - \boldsymbol{\eta}_1^{(j)}\|_2^2, \quad (5)$$

$$\mathbf{u}_1^{(j+1)} = \arg \min_{\mathbf{u}_1} \frac{\nu_0}{2} \|\mathbf{u}_0^{(j)} - \mathbf{C}\mathbf{u}_1 - \boldsymbol{\eta}_0^{(j)}\|_2^2 + \frac{\nu_1}{2} \|\mathbf{u}_1 - \mathbf{s}^{(j+1)} - \boldsymbol{\eta}_1^{(j)}\|_2^2, \quad (6)$$

$$\mathbf{u}_0^{(j+1)} = \arg \min_{\mathbf{u}_0} \frac{\lambda}{2} \|\mathbf{B}\mathbf{u}_0\|_2^2 + \frac{\nu_0}{2} \|\mathbf{u}_0 - \mathbf{C}\mathbf{u}_1^{(j+1)} - \boldsymbol{\eta}_0^{(j)}\|_2^2 \quad (7)$$

Equations (5) and (7) have simple closed-form solutions involving the inversion of diagonal matrices (see Steps 1 and 5 in Figure 2). The structure of \mathbf{C} makes the closed-form solution to (6) appear more complicated to compute:

$$\mathbf{u}_1^{(j+1)} = \left[\mathbf{C}^H \mathbf{C} + \frac{\nu_1}{\nu_0} \mathbf{I} \right]^{-1} \left(\mathbf{C}^H (\mathbf{u}_0^{(j)} - \boldsymbol{\eta}_0^{(j)}) + \frac{\nu_1}{\nu_0} (\mathbf{s}^{(j+1)} + \boldsymbol{\eta}_1^{(j)}) \right). \quad (8)$$

However, since $\mathbf{C}^H \mathbf{C}$ is block circulant with circulant blocks, $\mathbf{C}^H \mathbf{C} = \mathbf{Q}^H \boldsymbol{\Phi} \mathbf{Q}$ where \mathbf{Q} is a DFT matrix and $\boldsymbol{\Phi}$ is a diagonal matrix containing the spectrum of the convolution kernel of $\mathbf{C}^H \mathbf{C}$. Substituting this reformulation into (8) yields an exact, non-iterative solution (Step 3 in Figure 2). This solution is much simpler to compute because $\boldsymbol{\Phi}_2$ is a diagonal matrix and \mathbf{Q} can be implemented with a fast Fourier transform (FFT).

Updating the Lagrange multipliers, $\boldsymbol{\eta}$, between each alternating minimization step has been shown to increase the convergence rate of several AL based algorithms [11]. We therefore combine the previous alternating minimization steps with this updating scheme to obtain AL-Circ, our proposed AL estimation algorithm shown in Figure 2.

2.4. Parameter Selection

Our proposed AL method requires that we specify values for the convergence parameters ν_0 and ν_1 . Following [10], we determine the parameter values using the condition numbers of the matrices requiring inversion in the alternating minimization steps: \mathbf{B}_2 , $\boldsymbol{\Phi}_2$, and \mathbf{D}_2 as defined in Figure 2. If we normalize and mask the body coil image before performing the estimate, the condition number of \mathbf{D}_2 ($\kappa(\mathbf{D}_2)$) will not depend on the data. Thus, we set our parameters by considering the condition numbers of the other two matrices. Through extensive experimentation, we found that setting ν_0 such that $\kappa(\mathbf{B}_2) \in [250, 500]$ and then ν_1 such that $\kappa(\boldsymbol{\Phi}_2) \in [200, 2000]$ provided good convergence rates for a wide variety of data sets.

AL-Circ
Initialize: $\mathbf{u}_1^{(0)} = \mathbf{s}^{(0)}$, $\mathbf{u}_0^{(0)} = \mathbf{C}\mathbf{u}_1^{(0)}$, $\boldsymbol{\eta}_0^{(0)} = \mathbf{0}$, $\boldsymbol{\eta}_1^{(0)} = \mathbf{0}$, and $j = 0$.
Set $\mathbf{D}_2^{-1} = [\mathbf{D}^H \mathbf{D} + \nu_1 \mathbf{I}]^{-1}$ and $\mathbf{z}_2 = \mathbf{D}^H \mathbf{z}$.
Set $\mathbf{B}_2^{-1} = \begin{bmatrix} \lambda & \\ & \nu_0 \mathbf{B}^H \mathbf{B} + \mathbf{I} \end{bmatrix}^{-1}$.
Set $\boldsymbol{\Phi}_2^{-1} = [\boldsymbol{\Phi} + \frac{\nu_1}{\nu_0} \mathbf{I}]^{-1}$.
Repeat until stop criterion is achieved:
1. $\mathbf{s}^{(j+1)} = \mathbf{D}_2^{-1} (\mathbf{z}_2 + \nu_1 [\mathbf{u}_1^{(j)} - \boldsymbol{\eta}_1^{(j)}])$,
2. $\boldsymbol{\eta}_1^{(j+1/2)} = \boldsymbol{\eta}_1^{(j)} - (\mathbf{u}_1^{(j)} - \mathbf{s}^{(j+1)})$,
3. $\mathbf{u}_1^{(j+1)} = \mathbf{Q}^H \boldsymbol{\Phi}_2^{-1} \mathbf{Q}$ $(\mathbf{C}^H (\mathbf{u}_0^{(j)} - \boldsymbol{\eta}_0^{(j)}) + \frac{\nu_1}{\nu_0} (\mathbf{s}^{(j+1)} + \boldsymbol{\eta}_1^{(j+1/2)}))$,
4. $\boldsymbol{\eta}_0^{(j+1/2)} = \boldsymbol{\eta}_0^{(j)} - (\mathbf{u}_0^{(j)} - \mathbf{C}\mathbf{u}_1^{(j+1)})$,
5. $\mathbf{u}_0^{(j+1)} = \mathbf{B}_2^{-1} (\mathbf{C}\mathbf{u}_1^{(j+1)} + \boldsymbol{\eta}_0^{(j+1/2)})$,
6. $\boldsymbol{\eta}_0^{(j+1)} = \boldsymbol{\eta}_0^{(j+1/2)} - (\mathbf{u}_0^{(j+1)} - \mathbf{C}\mathbf{u}_1^{(j+1)})$,
7. $\boldsymbol{\eta}_1^{(j+1)} = \boldsymbol{\eta}_1^{(j+1/2)} - (\mathbf{u}_1^{(j+1)} - \mathbf{s}^{(j+1)})$,
8. $j = j + 1$.

Fig. 2. AL-Circ algorithm with intermediate Lagrange multiplier updating (Steps 2 and 4). Note that $\mathbf{C}\mathbf{u}_1^{(j+1)}$ only needs to be computed once per iteration.

3. RESULTS

We evaluated our proposed sensitivity estimation method on real breast phantom data. Since the accuracy of similar statistical estimators has been established [3], we focused on comparing the convergence properties of our AL algorithm with those of a CG approach to (1). To ensure a fair comparison, we also implemented the CG method with a circulant preconditioner:

$$\mathbf{P}_C = \mathbf{Q}^H (\mathbf{I} + \lambda \boldsymbol{\Omega}) \mathbf{Q}, \quad (9)$$

where $\boldsymbol{\Omega}$ is a diagonal matrix containing the spectrum of the convolution kernel of $\mathbf{R}^H \mathbf{R}$ [12].

We evaluated the following algorithms: CG, PCG with a circulant preconditioner (PCG-Circ), AL-Circ, and AL-Circ without intermediate updating (AL-Circ-NI). All of the algorithms were initialized with a zero estimate, i.e., $\mathbf{s}^{(0)} = \mathbf{0}$. We implemented the algorithms in MATLAB (The MathWorks, Natick, MA, USA) and ran the experiments on a PC with a 2.66 GHz, quad-core Intel Xeon CPU.

We compared the convergence properties of the algorithms using the normalized ℓ_2 -distance between the current estimate, $\mathbf{s}^{(j)}$, and the converged estimate, $\hat{\mathbf{s}}$:

$$\mathcal{D}(\mathbf{s}^{(j)}) = \frac{\|\mathbf{s}^{(j)} - \hat{\mathbf{s}}\|_2}{\|\hat{\mathbf{s}}\|_2}. \quad (10)$$

To facilitate the evaluation of our algorithms, we restricted ourselves to a small 2D problem so that we could use Cholesky factorization to determine a non-iterative solution to (1). Using this non-iterative solution for $\hat{\mathbf{s}}$ avoids favoring a specific iterative algorithm.

3.1. Cost Function Setup

In defining the estimation problem, (1), we used a second-order finite differencing matrix for \mathbf{R} as it resulted in more accurate sensitivity



Fig. 3. The magnitude of the breast phantom body coil image.

estimates than both first-order and fourth-order finite differences (results not shown). We determined the mask, \mathbf{m} , by thresholding the body coil image, \mathbf{y} , so that the majority of voxels in the object support were included, while limiting the number of noisy, non-object voxels. To determine the optimal regularization coefficient, λ , we first estimated the coil sensitivities using the CG method and several values of λ . We then performed two-fold accelerated SENSE reconstructions [1] using each set of estimated sensitivities and compared the resulting images to the body coil image. We selected $\lambda = 2^5$ as its corresponding reconstructed image had minimal artifacts and matched closely to the body coil image.

We selected the AL-Circ parameter values so that $\kappa(\mathbf{B}_2) = 265$ and $\kappa(\boldsymbol{\Phi}_2) = 450$. These parameter values were also used for AL-Circ-NI.

3.2. Breast Phantom Data

We acquired breast phantom data using four surface coils and one body coil on a Philips 3T scanner ($T_R = 4.6$ ms, $T_E = 1.7$ ms, matrix = 384×96). We then reconstructed the corresponding four surface coil images and one body coil image using an inverse FFT, Figures 3 and 4(a). Note that this data set presents several challenges for sensitivity estimation due to the placement of coils near the center of the field-of-view (FOV) and because of the large regions of low signal both within and outside the object.

We estimated the coil sensitivities using our proposed AL methods and the CG methods. We ran 20 000 iterations of each algorithm to ensure that convergence was achieved. The resulting estimates were all close to one another, converging to within single precision of the Cholesky factorization based estimate, $\hat{\mathbf{s}}$. Figure 4(b) presents the estimated coil sensitivities generated by AL-Circ. The convergence rates of the algorithms were similar for all four coils and thus we present the results for one representative coil. Figure 5 plots $\mathcal{D}(\mathbf{s}^{(j)})$ with respect to time for the far right coil in Figure 4. AL-Circ was the fastest algorithm, reaching $\mathcal{D}(\mathbf{s}^{(j)}) = 0.1\%$ in 1100 iterations and approximately 50 s. The same AL algorithm without intermediate updating, AL-Circ-NI, required 2000 iterations and 90 s. The CG based algorithms took longer, with PCG-Circ requiring 2200 iterations and 110 s and standard CG needing nearly 10 000 iterations and 425 s.

4. DISCUSSION

The final estimates generated by minimizing the cost function in (1) are smooth like true coil sensitivities. The ability to estimate the sensitivities of surface coils oriented between the breasts and within the FOV demonstrates the flexibility of the statistical estimation method. Specifically, our method captured the increased sensitivity in the middle of the FOV and accurately estimated the decreasing sensitivity over both breasts for these coils.

Our AL based method and its variation converged faster than the CG based methods. Most significantly, AL-Circ converged in approximately half the time of PCG-Circ and one eighth the time



Fig. 4. The magnitude of the (a) surface coil images (top row) and the (b) corresponding sensitivity estimates (bottom row).

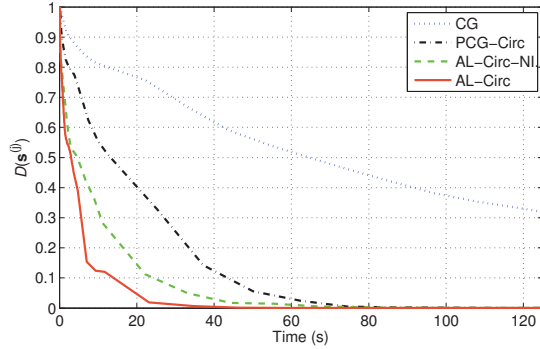


Fig. 5. Plots of the normalized ℓ_2 -distance between $\mathbf{s}^{(j)}$ and $\hat{\mathbf{s}}$, $\mathcal{D}(\mathbf{s}^{(j)})$, with respect to time for the far right coil in Figure 4.

of traditional CG. It should also be noted that a nearly two fold improvement in convergence rate was obtained for the AL algorithm by updating the Lagrange multipliers between alternating minimization steps.

Our proposed algorithm is highly robust to the particular choice of convergence parameter values. In fact, the same parameter values were used in experiments on a simulated brain data set with similar results (not shown). Furthermore, the optimal parameter values do not depend on the surface coil image. Thus, one only has to determine the optimal parameters for a single coil of a multi-coil array.

While there is no guarantee of convergence for our proposed algorithm, it has converged in every experiment we have attempted. We are currently investigating an alternating direction method of multipliers (ADMM) [13] adaptation of AL-Circ that has a proof of convergence.

5. CONCLUSIONS

We have presented a novel augmented Lagrangian based sensitivity estimation method that converges in half the time of the traditional method, PCG. These time savings are particularly significant when working with large coil arrays. Our proposed AL method separates the finite differencing matrix into components with more exploitable structures. This approach allows for a final algorithm with exact alternating minimization steps. Furthermore, we were able to significantly accelerate our AL algorithm by updating the Lagrange multipliers between minimization steps. Similar AL algorithms could be applied to other estimation problems with quadratic regularization (e.g., [14]); however, this remains an open problem.

6. REFERENCES

- [1] K. P. Pruessmann, M. Weiger, M. B. Scheidegger, and P. Boesiger, "SENSE: sensitivity encoding for fast MRI," *Mag. Res. Med.*, vol. 42, no. 5, pp. 952–62, Nov. 1999.
- [2] S. O. Schönberg, O. Dietrich, M. F. Reiser, and A. L. Baert, *Parallel Imaging in Clinical MR Applications*, Medical Radiology Diagnostic Imaging Series. Springer, 2007.
- [3] S. L. Keeling and R. Bammer, "A variational approach to magnetic resonance coil sensitivity estimation," *Applied Mathematics and Computation*, vol. 158, no. 2, pp. 53–82, Nov. 2004.
- [4] D. J. Larkman and R. G. Nunes, "Parallel magnetic resonance imaging," *Phys. Med. Biol.*, vol. 52, no. 7, pp. R15–R55, Apr. 2007.
- [5] R. Bammer, R. Stollberger, M. J. Augustin, T. Seifert, S. Strasser-Fuchs, P. Wach, H. P. Hartung, and F. Fazekas, "Parallel imaging strategies for high-speed magnetic resonance diffusion imaging," in *Proc. SPIE 3978*, 2000, vol. 12.
- [6] F. H. Lin, Y. J. Chen, J. W. Belliveau, and L. L. Wald, "A wavelet-based approximation of surface coil sensitivity profiles for correction of image intensity inhomogeneity and parallel imaging reconstruction," *Hum. Brain Map.*, vol. 19, no. 2, pp. 96–111, Mar. 2003.
- [7] M. A. G. Ballester, Y. Machida, Y. Kassai, Y. Hamamura, and H. Sugimoto, "Robust estimation of coil sensitivities for RF subencoded acquisition techniques," in *Proc. Intl. Soc. Mag. Res. Med.*, 2001, p. 799.
- [8] R. Bammer, M. Auer, S. L. Keeling, M. Augustin, L. A. Stables, R. W. Prokesch, R. Stollberger, M. E. Moseley, and F. Fazekas, "Diffusion tensor imaging using single-shot SENSE-EPI," *Mag. Res. Med.*, vol. 48, no. 1, pp. 128–36, July 2002.
- [9] M. J. Allison and J. A. Fessler, "An augmented Lagrangian method for MR coil sensitivity estimation," in *Proc. Intl. Soc. Mag. Res. Med.*, 2011, p. 2881.
- [10] S. Ramani and J. A. Fessler, "Parallel MR image reconstruction using augmented Lagrangian methods," *IEEE Trans. Med. Imag.*, vol. 30, no. 3, pp. 694–706, Mar. 2011.
- [11] R. Glowinski and P. L. Tallec, *Augmented Lagrangian and operator-splitting methods in nonlinear mechanics*, Soc. Indust. Appl. Math., 1989.
- [12] R. H. Chan, "Circulant preconditioners for Hermitian Toeplitz systems," *SIAM J. Matrix. Anal. Appl.*, vol. 10, no. 4, pp. 542–50, 1989.
- [13] J. Eckstein and D. P. Bertsekas, "On the Douglas-Rachford splitting method and the proximal point algorithm for maximal monotone operators," *Mathematical Programming*, vol. 55, no. 1-3, pp. 293–318, Apr. 1992.
- [14] A. K. Funai, J. A. Fessler, D. T. B. Yeo, V. T. Olafsson, and D. C. Noll, "Regularized field map estimation in MRI," *IEEE Trans. Med. Imag.*, vol. 27, no. 10, pp. 1484–94, Oct. 2008.